



Optical properties of Pr implanted GaN epilayers and $\text{Al}_x\text{Ga}_{1-x}\text{N}$ alloys

C.J. Ellis ^a, R.M. Mair ^a, J. Li ^a, J.Y. Lin ^a, H.X. Jiang ^{a,*}, J.M. Zavada ^b,
R.G. Wilson ^c

^a Department of Physics, Kansas State University, Manhattan, KS, 66506-2601, USA

^b US ARL-European Research Office, London NW1 5TH, UK

^c Consultant, Stevenson Ranch, CA, 91381, USA

Abstract

It has been shown recently that III–V nitrides serve as a good host for rare earth elements and have many potential applications in optical communications. Most work in rare earth implanted III-nitride materials so far has been focused on GaN, while AlGaN alloys should have advantages over GaN due to wider energy band gap. In this work, photoluminescence (PL) spectroscopy was used to investigate praseodymium (Pr) related transitions in Pr-implanted GaN and $\text{Al}_x\text{Ga}_{1-x}\text{N}$ ($0.15 < x < 0.33$). The GaN epilayers and $\text{Al}_x\text{Ga}_{1-x}\text{N}$ alloys were rapid thermally annealed in nitrogen ambient to facilitate recovery from implantation related damage. We observed narrow PL emission bands near 526, 650, 950, 1100 and 1300 nm. The dependence of PL emission including line width, peak position and emission intensity on sample temperature, excitation intensity, aluminum concentration and annealing conditions were systematically studied. We found that PL intensity increases with annealing time and temperature. In contrast to GaN epilayers, different behaviors have been observed in the AlGaN host alloys. © 2001 Elsevier Science B.V. All rights reserved.

Keywords: AlGaN alloys; Praseodymium; Ion implantation; Photoluminescence

1. Introduction

III–V semiconductors have proven to be very versatile and have been incorporated into many new devices. One particularly important III–V material is the III-nitride, which has been the subject of intensive investigation in recent years [1–6] and has been widely studied recently for applications in two areas: (1) optical devices, including blue-UV light emitting diodes (LED) and blue-UV laser diodes; [7–11] (2) electronic devices, including devices operating in hostile environments such as high temperatures and high radiation doses and under extreme conditions such as high frequency and high power. Erbium (Er) and Praseodymium (Pr)-implanted materials are of particular interest to the optical communication industry because they exhibit emission at the wavelengths 1540 and

1300 nm, corresponding to the minimum transmission loss and minimum dispersion within optical fibers, respectively. Studies of Er^{3+} implanted semiconductors have shown that thermal quenching of Er^{3+} emission decreases with increasing band gap of the host material [12]. This phenomenon has naturally led recent research efforts toward rare earth doping within the wide band gap III-nitride semiconductor system [13–20].

2. Experimental details

Pr was implanted into MOCVD grown GaN and AlGaN samples at a dose of $5.7 \times 10^{13} \text{ cm}^{-3}$ and energy of 300 keV. After implantation, the samples were cut into small pieces. The GaN samples were annealed in an MOCVD reactor for 10 min in a nitrogen ambient at various temperatures ranging from 750 to 1050°C. The AlGaN samples were annealed in a rapid thermal annealing furnace in a nitrogen ambient for 150 s at various temperatures ranging from 750 to

* Corresponding author. Tel.: +1-785-232-1627; fax: +1-785-776-8105.

E-mail address: jiang@phys.ksu.edu (H.X. Jiang).

1150°C. The optical properties of Pr-implanted GaN and AlGaN films have been studied by PL spectroscopy. The excitation source consisted of 290 nm laser pulses with 10 ps width and 9.5 MHz repetition rate. PL emissions below 650 nm were collected and analyzed with a 1.3 m grating monochromator equipped with a microchannel plate photomultiplier tube used in a single photon counting mode. The PL emissions over 800 nm were collected and analyzed with a 0.3 m monochromator equipped with a thermoelectrically cooled InGaAs photodiode detector.

3. Results

In Fig. 1(a), we plot the room temperature and 10 K PL spectra over the range of 640–680 nm for a Pr-implanted GaN sample, which was annealed at 1050°C for 10 min. At least five distinct atomic transitions can be seen in this plot and the room temperature line-widths are clearly much smaller than expected for typical impurity related transitions in GaN. Furthermore, the lines show virtually no temperature related wavelength shift as one might expect for band or impurity related transitions in semiconductors. These narrow PL emission lines appear related to 4f intrashell transitions of the Pr^{3+} ion. The closely spaced multiplet of lines originate from the crystal field splitting of otherwise forbidden transitions. The PL emission from the Pr-im-

planted GaN samples exhibited a strong dependence on sample annealing temperature. The integrated PL intensity as a function of annealing temperatures for the most intense pair of transitions at 650.5 and 652.5 nm is plotted in Fig. 1(b). We found that PL intensity increases exponentially with annealing temperature up to the temperature of 1050°C and further increase in annealing temperature caused a degradation in PL intensity in nitrogen ambient. However, when annealing GaN samples in an ammonia ambient, PL intensity was greatly enhanced for annealing temperatures up to 1150°C. These results suggested that thermal degradation of the GaN host material becomes prevalent and the complete Pr^{3+} activation was not yet achieved at a temperature of 1050°C in nitrogen ambient. It is clear from Fig. 1 that there is no significant thermally induced degradation of PL efficiency up to room temperature. Emissions at longer wavelengths than 650 nm showed no dependence upon annealing temperature.

Some of the GaN samples of the current study were co-implanted with Pr and O and then annealed at temperatures between 800 and 1000°C in order to investigate the effect of oxygen impurities on the Pr^{3+} -related PL. For all the annealing temperatures investigated, the Pr + O implanted samples exhibited reduced efficiency. The samples were annealed in a manner identical to the Pr implanted GaN samples, in which they were placed in a nitrogen ambient, and the samples exhibited less PL intensity near 650 nm than

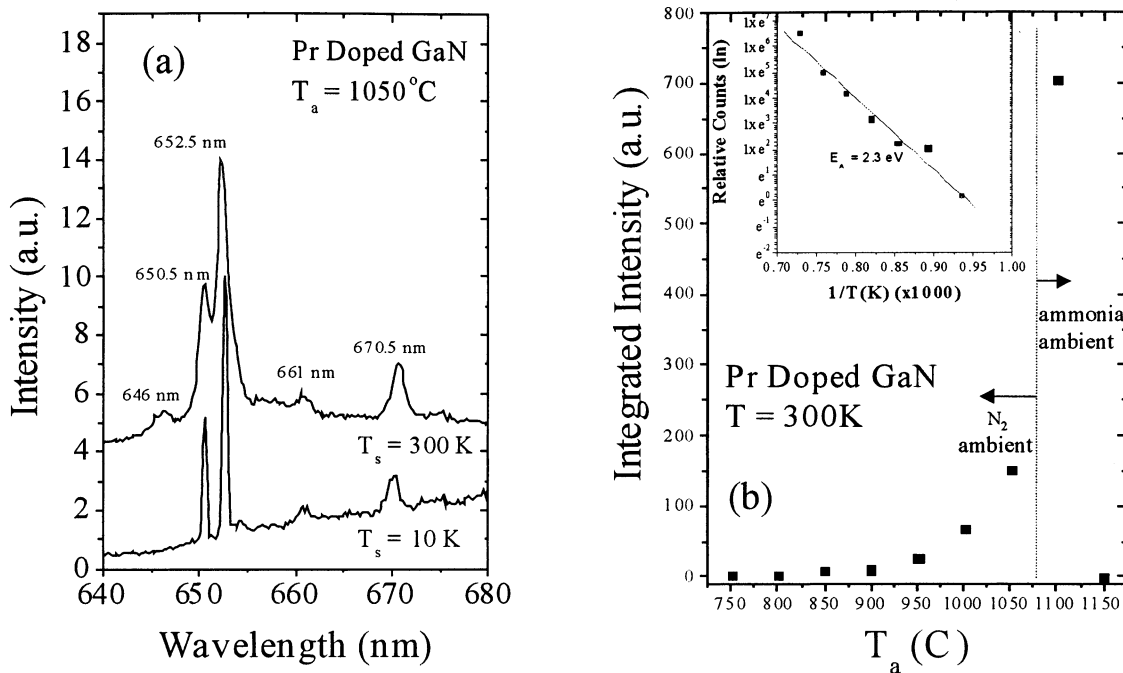


Fig. 1. (a) PL spectra measured at 10 and 300 K from the Pr-implanted GaN sample annealed at 1050°C. The spectra are vertically displaced for a clear presentation. The spectra show ${}^3\text{P}_0\text{--}{}^3\text{F}_2$ transitions of the Pr^{3+} ion in GaN near 650 nm. (b) The dependence of the integrated room temperature PL emission intensity between 647.5 and 644 nm on sample annealing temperature measured at 300 K. The inset is the Arrhenius plot of the emission intensity and a least squares fit of exponential form implies a thermal activation energy of 2.3 eV for the Pr-implanted GaN.

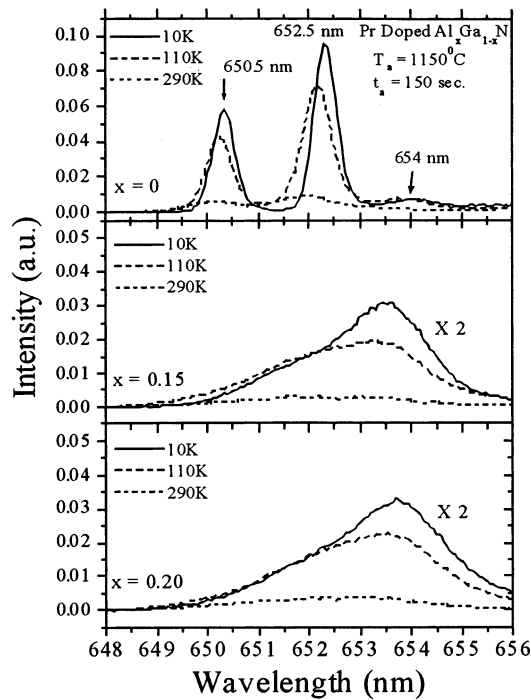


Fig. 2. PL Spectra measured at three representative temperatures 10, 110 and 290 K for the Pr-implanted GaN epilayer, the $\text{Al}_{0.15}\text{Ga}_{0.85}\text{N}$ alloy, and the $\text{Al}_{0.20}\text{Ga}_{0.80}\text{N}$ alloy.

the samples implanted with only Pr. It was found that oxygen incorporation reduces the PL intensity for the region of interest by up to 50%. To compare our results to earlier studies of Er-implanted Si materials, which suggested that oxygen incorporation can enhance the Er^{3+} PL efficiency [12,13,21], we observe a modest degradation of Pr^{3+} -related PL efficiency. Our results are consistent with a recent study [20], where little Er^{3+} PL efficiency dependence on oxygen co-doping was seen in Er-implanted GaN under an above band gap excitation condition. Temperature dependence studies were conducted for the set of Pr + O samples and we found a similar trend of exponential increase in PL intensity with temperatures up to 1000°C. The resulting thermal activation energy was found to be around 1.19 eV.

For the AlGaIn samples, rapid thermal annealing was employed. In this case, the PL intensity increases exponentially with annealing temperature up to a temperature of 1150°C. The results shown here are for AlGaIn samples annealed at $T_{\text{ann}} = 1150^\circ\text{C}$ for a time $t_{\text{ann}} = 150$ s. AlGaIn with various aluminum concentrations, ranging 15, 20, 28 and 33% were used for this study. PL emission was observed at 300, 526, 650, 950, 1100 and 1300 nm for Pr implanted AlGaIn. The five distinct transitions other than 300 nm line can be seen in the room temperature PL spectra. The PL at the 300 nm region corresponds to the band edge transition of the AlGaIn band gap. The 526 nm emission line was enhanced in AlGaIn over GaN.

The spectral region that proved most interesting for our samples was the 650 nm region. A systematic study of temperature dependence with Al content was therefore performed. The PL emission in the 650 nm region is shown in Fig. 2, which was only observable for AlGaIn samples with low concentrations of Al.

The focus was thus upon these AlGaIn samples having the most PL intensity in the 650 nm region, which were the 15 and 20% Al samples. It can be seen that the sample with $x = 0$ has three peaks at 650.5, 652.5 and 654 nm. On the other hand, the emission at 650 and 653 nm was suppressed and only one broad peak around 654 nm was seen in AlGaIn alloys. The 650 nm peaks are related to the ${}^3\text{P}_0\text{--}{}^3\text{F}_2$ atomic transitions [22]. We found that the peak positions showed a small shift with temperature. In the AlGaIn epilayers, we were able to fit a double Gaussian peak distribution. It appears that the larger of these fitted peaks has the same origin as the smallest peak (654 nm) in the GaN epilayer and the smaller of the fitted peaks correlates to the middle peak (652.5 nm) from the GaN sample. The sample temperature dependence of PL intensity can be fitted with equation:

$$I(T) = I_0/[1 + C\exp(-E_a/kT)], \quad (1)$$

where C is a constant, E_a is the thermal activation energy, k is the Boltzman constant, and T in the sample temperature. The experimental result together with the fitted curves is shown in Fig. 3 for three different Al contents. No systematic dependence of E_a on the Al content was seen in this case.

The rest of the transitions in the 950, 1100 and 1330 nm regions are represented in Fig. 4. The results shown in Fig. 4 suggested that Al content plays a minor role in the integrated intensity of these emission lines.

4. Conclusions

In this work, we have studied optical transitions in Pr implanted GaN epilayers and AlGaIn alloys by photoluminescence spectroscopy. The effects of rare earth doping, alloy composition and annealing conditions were systematically studied. Basic transitions involving atomic energies of Pr ions have been identified in these materials.

For the Pr implanted GaN epilayers, we found that, (i) the optical transitions in the various regions demonstrated strong dependence on annealing conditions; (ii) the thermal quenching of the Pr related emission was suppressed in samples annealed at 1050°C; (iii) Oxygen incorporation into Pr implanted GaN samples reduced PL intensity by about a factor of 2; and (iv) Pr + O samples demonstrated similar thermal stability as Pr only implanted samples.

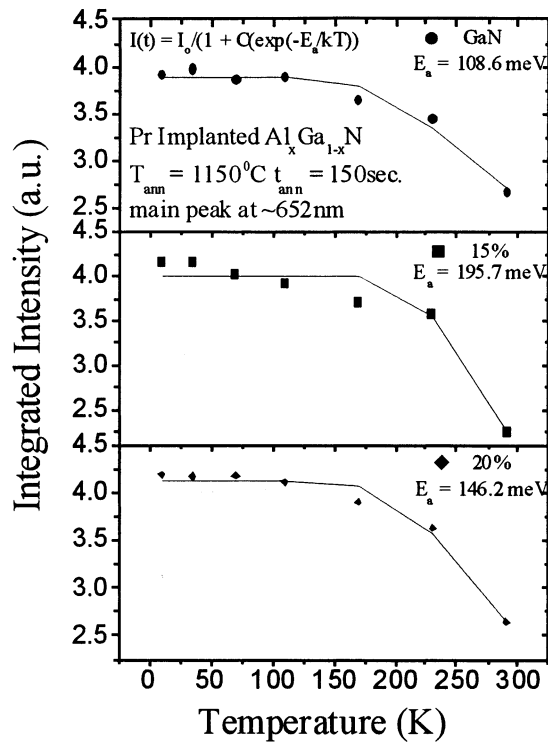


Fig. 3. PL integrated intensity vs. temperature in the 650 nm region by Eq. (1). The equation of fitting reveals the thermal activation energy for the Pr-implanted GaN epilayer and $\text{Al}_x\text{Ga}_{1-x}\text{N}$ alloys studied.

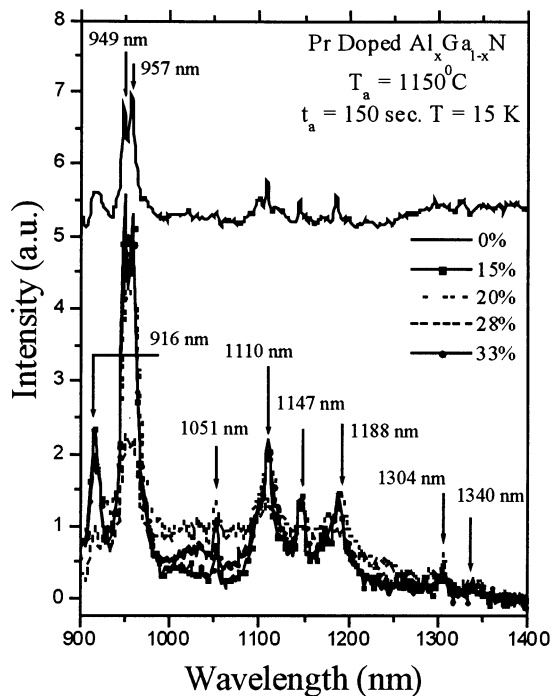


Fig. 4. PL spectra measured at 15 K for the Pr-implanted GaN epilayer and the $\text{Al}_x\text{Ga}_{1-x}\text{N}$ alloys. The spectra are vertically displaced for a clear presentation.

For the Pr implanted AlGaIn alloys, we found that, (i) the ideal annealing conditions involved a temperature of 1150°C in nitrogen ambient for 150 s; (ii) increased Al content enhanced the 526 nm transition line while the 650 and 652 nm emission lines were reduced and the IR region was unaffected; and (iii) emission lines around 650 nm were completely suppressed in $\text{Al}_x\text{Ga}_{1-x}\text{N}$ with $x > 0.20$.

Acknowledgements

The research at Kansas State University is supported by ARO.

References

- [1] Wide Band Gap Semiconductors, edited by T.D. Moustakas, J.I. Pankove, Y. Hamakawa, Mater. Res. Soc. Symp. Proc. (MRS, Pittsburgh, 1992), 242.
- [2] S. Strike, M.E. Lin, H. Morkoc, This Solid Films 231 (1993) 197.
- [3] J.I. Pankove, Mater. Res. Soc. Symp. Proc. 97 (1987) 409.
- [4] S. Nakamura, M. Senoh, T. Mukai, Jpn. J. Appl. Phys. 32 (1993) L8.
- [5] S.N. Mohammad, H. Morkoc, Photon Quantum Electronics, 20 (1996) 361.
- [6] Gallium Nitride and Related Materials, edited by F.A. Ponce, R.D. Dupuis, S. Nakamura, J.A. Edmond, Mater. Res. Soc. Symp. Proc. (MRS, Pittsburgh, 1992), 395.
- [7] H. Morkoc, S. Strite, G.B. Gao, M.E. Lin, B. Sverdlov, M. Burns, J. Appl. Phys. 76 (1994) 1363.
- [8] M.A. Khan, M.S. Shur, J.N. Kuznia, Q. Chen, J. Burn, W. Schaff, Appl. Phys. Lett. 66 (1995) 1083.
- [9] S. Nakamura, T. Mukai, M. Senoh, Appl. Phys. Lett. 64 (1994) 1687.
- [10] S. Nakamura, M. Senoh, M. Iwasa, S. Nagahama, Jpn. J. Appl. Phys. 34 (1995) L797.
- [11] S. Nakamura, M. Senoh, S. Nagahama, N. Iwasa, T. Yamada, T. Matsushita, Y. Sugimoto, H. Kiyoku, Appl. Phys. Lett. 68 (1996) 2105.
- [12] P.N. Favennec, H. L'Haridon, M. Salvi, D. Moutonnet, Y.L. Guillou, Electron Lett. 25 (1989) 718.
- [13] J.M. Zavada, D. Zhang, Solid-State Electron 38 (1995) 1285.
- [14] R.G. Wilson, R.N. Schwartz, C.R. Abernathy, S.J. Pearton, N. Newman, M. Rubin, T. Fu, J.M. Zavada, Appl. Phys. Lett. 65 (1994) 992.
- [15] J.T. Torvik, R.J. Feuerstein, J.L. Pankove, C.H. Qui, F. Namavar, Appl. Phys. Lett. 69 (1996) 2098.
- [16] J.D. MacKenzie, C.R. Abernathy, S.J. Pearton, U. Hommerich, X. Wu, R.N. Schwartz, R.G. Wilson, J.M. Zavada, Appl. Phys. Lett. 69 (1996) 2083.
- [17] S. Kim, S.J. Rhee, D.A. Turnbull, E.E. Reuter, X. Li, J.J. Coleman, S.G. Bishop, Appl. Phys. Lett. 71 (1997) 231.
- [18] D.M. Hansen, R. Zhang, N.R. Perkins, S. Safvi, L. Zhang, K.L. Bray, T.F. Kuech, Appl. Phys. Lett. 72 (1997) 1244.
- [19] R. Birkhahn, M. Garter, A.J. Steckl, Appl. Phys. Lett. 74 (1999) 2161.
- [20] L.C. Chao, A.J. Steckl, Appl. Phys. Lett. 74 (1999) 2364.
- [21] J. Michel, L.L. Benton, R.F. Ferrante, D.C. Jacobsen, D.J. Eaglesham, E.A. Fitzgerald, Y.-H. Xie, J.M. Poate, L.C. Kimerling, J. Appl. Phys. 70 (1991) 2672.
- [22] A.A. Kaminskii, Laser Crystals, Springer, Berlin, 1981.